



# Physical layer amendments for MIMO features in 802.11a

Ralf Eickhoff<sup>1</sup>, Klaus Tittelbach-Helmrich<sup>2</sup>, Michael Wickert<sup>1</sup>, Jens Wagner<sup>1</sup>, Uwe Mayer<sup>1</sup>, Victor Elvira<sup>3</sup>, Jesús Ibáñez<sup>3</sup>, Zoran Stamenkovic<sup>2</sup>, Frank Ellinger<sup>1</sup>

<sup>1</sup>*Technische Universität Dresden, Helmholtzstraße 18, Dresden, 01062, Germany*

*Email: {Ralf.Eickhoff, Michael.Wickert, Jens.Wagner, Uwe.Mayer, Frank.Ellinger}@tu-dresden.de*

<sup>2</sup>*IHP, Im Technologiepark 25, Frankfurt (Oder), 15236, Germany*

*Email: {tittelbach, stamenkovic}@ihp-microelectronics.com*

<sup>3</sup>*University of Cantabria, Plaza de la Ciencia, Santander, 39005, Spain*

*Email: {victorea, jesus}@gtas.dicom.unican.es*

**Abstract:** This paper presents enhancements in the physical layer of 802.11a wireless local area networks (WLANs) to support multiple-input multiple-output (MIMO) communication. In this approach, spatial diversity is exploited at the radio-frequency (RF) front-end by weighting the transmitted and the received signals using integrated circuits (ICs). Their optimum weight settings are derived by baseband algorithms based on the estimated MIMO channel response. Prototyping platforms are designed for baseband signal processing and RF transmission, which contain all key components for the RF-MIMO technique and 802.11a data transmission, respectively. The developed algorithms, computing platforms and ICs are successfully verified with respect to the RF-MIMO concept and their compatibility to 802.11a devices.

**Keywords:** MIMO, 802.11a, WLAN, wireless communications.

## 1. Introduction

Because MIMO concepts offer various performance improvements in wireless links, this technique was recently adopted in several standards such as 802.11n [1, 2], WiMAX or LTE/LTE-Advanced [3] for single- and multi-user scenarios. Thus, conventional links are not only improved in performance because of spatial diversity or multiplexing gain, but also new types of links are enabled in multi-user support.

However, mobile devices suffer from increased hardware costs, power consumption and devices sizes, because MIMO schemes are usually exploited in the baseband and, hence, parallel operating RF transceivers are required. If spatial diversity is utilised in the RF domain by adequately weighting the antenna signals after up-conversion at the transmitter (Tx) or before down-conversion at the receiver (Rx), the hardware overhead will be reduced in comparison to conventional approaches [4], i.e. several components of the analogue front-end can be shared among transceiver branches. Therefore, the component count, system costs, and power consumption will decrease for that RF-MIMO approach but still offering spatial features. Albeit there are some similarities to smart antennas or beamforming [5], amplitudes and phases are adjusted in the RF-MIMO concept with respect to the MIMO channel.

The RF-MIMO technology relies on weighting the RF signals in the analogue domain by vector modulators, those settings are derived by baseband algorithms. This signal processing must account for the special front-end architecture and a MIMO channel

estimation, because only a single up- and down-conversion path are used in the RF transceiver. More details about the concept and its performance for single- and multi-user scenarios can be found in [6-8].

This paper presents the physical layer design for enabling the RF-MIMO concept in 802.11a WLANs. The building blocks and key components were developed for the antenna array, the RF transceiver, the baseband processing, and the medium access control (MAC). These software and hardware parts are partitioned into different rapid prototyping platforms for testing and evaluating the concept, and they support the RF-MIMO technology as well as legacy 802.11a data transmission.

## 2. Physical layer architecture and partitioning

Several parts of the physical layer are changed to enable MIMO-based data transmission inherently in 802.11a WLANs. However, besides changes in the front-end architecture and the baseband processing further modifications up to the MAC are required for supporting legacy modes and standard compliant transmission.

The antenna array for the RF-MIMO approach is based on four microstrip-fed planar F-shaped monopoles. Each radiator is printed on a low cost FR4 substrate and supports multi-band operation in the 2.4 GHz and the 5.6 GHz frequency bands by using different resonant curls in its layout. The complete array is assembled for a laptop form factor by using a carrier substrate, i.e. an antenna holding structure, and further exploits polarisation diversity. The radiators are connected to the RF front-end by SMA cables, which are directly soldered at the antenna.

The RF front-end consists of two separated subsystems, Tx and Rx, located on opposite sides of a common PCB to minimise coupling between them. Each part employs four parallel branches in the RF domain for transmitting and receiving the OFDM signals, but uses only a single up- and down-conversion path. Finally, spatial diversity is exploited by weighting the RF signals using vector modulators at the RF domain, i.e. after splitting the up-converted signal at the Tx or before combining the received antenna signals into a single RF signal for down-conversion at the Rx, respectively. Therefore, the hardware overhead and the power consumption are reduced in comparison to conventional MIMO, but the transceiver's input and output signals are still compatible to any 802.11a baseband implementation.

Nevertheless, for optimally exploiting spatial diversity at the RF domain algorithms for beamformer selection, i.e. deriving the optimum weight configuration for the RF front-end, and MIMO channel estimation are required because 802.11a has not been specified for supporting MIMO transmission modes. Beamformer selection is based on optimising a dedicated cost function [7], which supports different performance metrics, e.g. maximising the signal-to-noise-ratio or the overall link capacity. For channel estimation, special training frames are transmitted, which are discarded by the baseband of legacy devices but recognised by the RF-MIMO baseband due to customised signal fields. This allows the Tx transmitting pilot signals, and the Rx determines the MIMO channel based on a least-square estimation operating in the frequency domain.

For the MAC, a RISC core executes the protocols, and it is enhanced with hardware accelerators for time critical operations. No changes are required on the MAC layer except of internal modifications in the computing platform features. As an example, the re-estimation of the MIMO channel must be initiated when the performance degrades. Moreover, compatibility to any mobile service or application is guaranteed by supporting the 802.11 MAC protocol and an 802.2 link layer control.

Figure 1 shows the architecture and the partitioning of the physical layer including all subsystems described above. The whole prototyping system is split into three printed circuit

boards (PCBs): MAC, baseband, and RF transceiver. The antenna array is separately optimised for laptop integration.

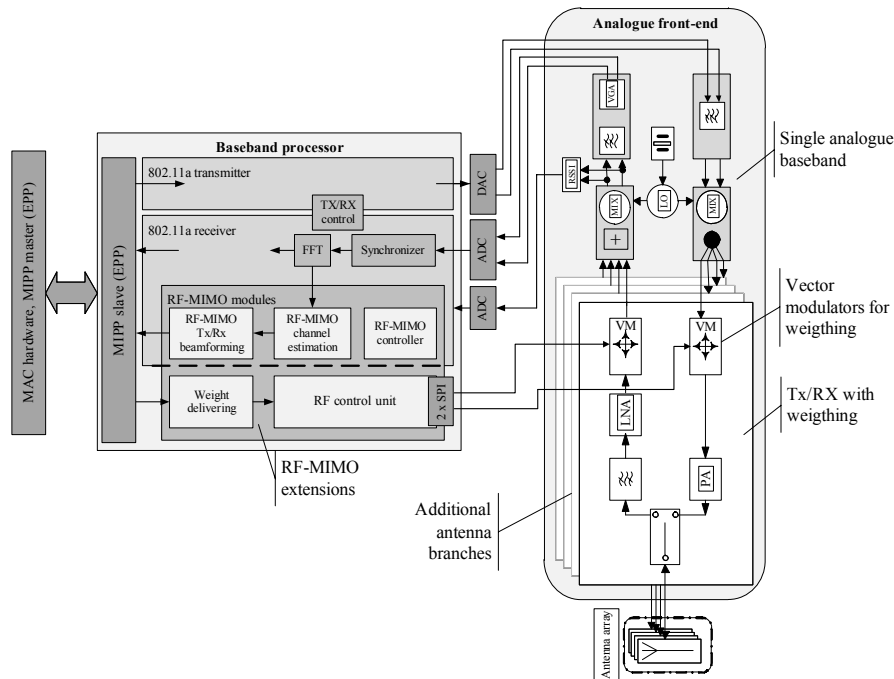


Figure 1 Physical layer concept and system partitioning.

### 2.1 Baseband prototyping platform

According to the RF-MIMO system architecture and partitioning (cf. Figure 1), prototyping of the 802.11a baseband and the MIMO extension is performed by a PCB, which includes a XILINX Virtex-V FPGA for signal processing, specific interfaces to the MAC PCMCIA card and the analogue front-end PCB. Figure 2 shows that prototyping board, which is 135 mm x 225 mm in size.

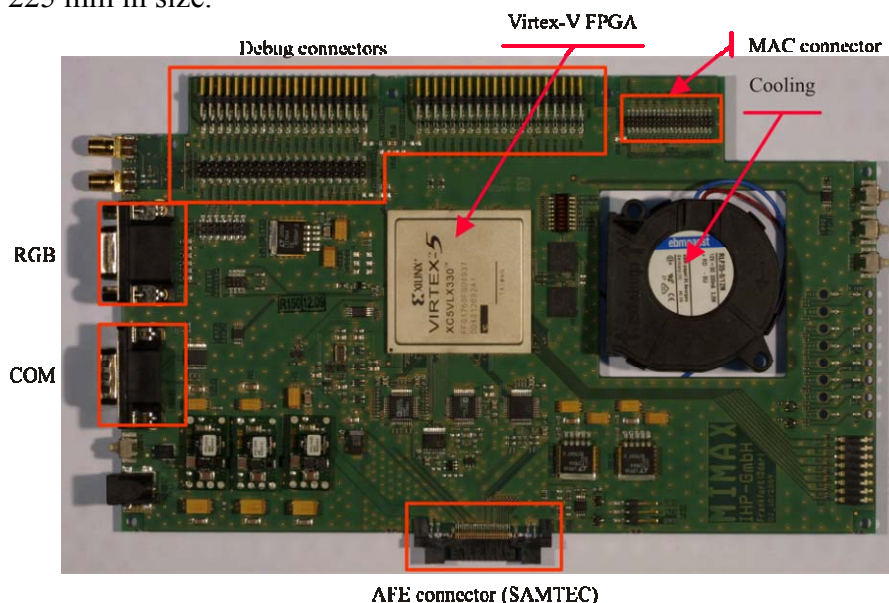


Figure 2 Baseband rapid prototyping PCB with Virtex-V FPGA.

A XILINX Virtex-V LX330 performs the signal processing for 802.11a operation in Tx and Rx direction, e.g. interleaver, mapper, IFFT, insertion of guard interval and preamble, synchroniser, FFT, demapper, deinterleaver and Virterbi decoder. The baseband processor

is enhanced with dedicated signal processing for MIMO channel estimation and beamformer selection. These RF-MIMO modules are only activated during exchanging RF-MIMO training frames between two stations.

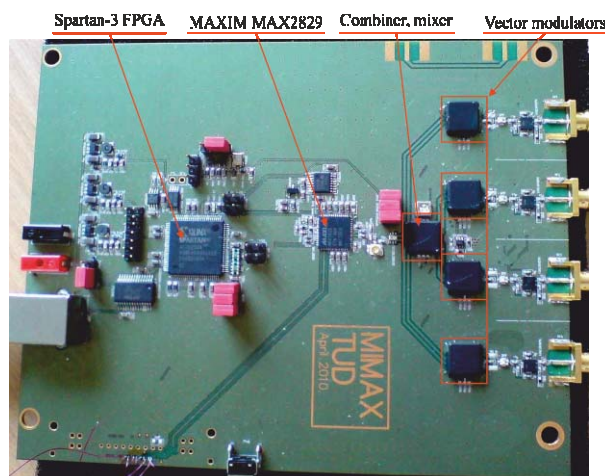
Further tasks of the baseband consist of controlling the RF transceiver settings and configuring the weighting circuitry at the RF domain. A dedicated control unit adjusts the basic parameters of the transceiver via a SPI, e.g. gain settings, channel number, etc., and it converts the determined weights of the baseband algorithms into control signals for the RF weighting circuitry. During this conversion, impairments of the analogue circuits such as non-linearities or inter-branch mismatch are compensated to minimise their effects on link performance.

The MAC board is connected by an enhanced parallel port (EPP), which is extended in its features to support higher throughputs. The RF front-end board uses a SAMTEC connector, which incorporates all control and data flow signals. The baseband board contains several analogue-to-digital-converters (ADCs) and digital-to-analogue-converters (DACs) to generate/sample the I- and Q-signals or to acquire a receive-signal-strength-indicator (RSSI) signal. Those components were selected based on the requirements with regard to resolution, bandwidth, and dynamic range.

Moreover, several supplementary interfaces are assembled on the PCB for debugging and testing, to program the FPGA or to store its configuration data in flash memory. Those interfaces enable different test modes including a standalone verification of that prototyping board without any MAC or RF transceiver. For example, the RGB port allows direct visualization of the constellation diagram on a computer monitor. For testing, additional boards, which either emulate the RF transceiver including the wireless channel or the MAC protocol, can be attached.

## 2.2 RF front-end board

The RF-MIMO analogue front-end is assembled on a PCB, which is shown in Figure 3. In its initial version, the board supports a 1x4-MIMO operation and the key components such as the vector modulators and the combining circuits were designed in a 0.25  $\mu\text{m}$  SiGe-BiCMOS technology. Those chips are mounted on the PCB together with an off-the-shelf WLAN IC (MAX2829) from MAXIM. Future redesigns will integrate the complete MIMO Tx and Rx functionality into two separate ICs<sup>1</sup>. The antennas are connected via SMA cables, which are directly soldered at the antenna input for improved matching, and for the baseband a SAMTEC connector is used (cf. Figure 2).



<sup>1</sup> Tx and Rx will consist of separated ICs to minimise coupling effects, e.g. preventing the power amplifiers of the Tx saturating the low-noise amplifiers at the Rx.

*Figure 3 PCB with analogue front-end based on hybrid components.*

The circuits for weighting the RF signals use vector modulators, which split an incoming signal into two orthogonal branches using an all-pass filter based phase shifter. Each of those signals is independently amplified by a variable gain amplifier before they are finally superposed. Because in its first design the vector modulator was developed also as a low-noise amplifier, this restricts the current implementation of the front-end board to 1x4-MIMO configurations supporting antenna selection at the Tx. The redesigned Tx uses optimised vector modulators, i.e. enabling 4x4-MIMO scenarios.

Moreover, the board contains the required combining circuits at the Rx. The combiner is based on common-base stages, which are connected to a common load. The combined signal is fed to a MAX2829 chip for further down-conversion. The more challenging dynamic range requirements, e.g. 12 dB higher input power range compared to legacy 802.11a, at the input of the MAX2829 chip are compensated by adjusting the combiner gain.

Either the front-end PCB can be controlled by the baseband board, e.g. adjusting the basic settings of the MAXIM IC and configuring the weighting circuitry, or it is configured for standalone operations. Therefore, a Spartan-3 FPGA is used on the board, which receives the control commands and the weights from the baseband and routes them to the components accordingly. In the standalone or testing mode, the FPGA configures the board itself and all commands from the baseband are dismissed. Furthermore, that FPGA will also be used on the PCB with the integrated Tx and Rx chips, which allows exchanging both boards in the system prototype because they support the same protocols and interfaces to the baseband and the antenna array.

Finally, several supplementary components for board operation, testing and debugging are assembled on the front-end PCB, which are required for FPGA programming, clock generation or power supply.

### **3. Prototype evaluation**

The described physical layer components, the baseband and the front-end board, can be configured to standalone operation and tested independently from the other subsystems. For testing the baseband board, the MAC is replaced by a control terminal program running on a PC, which is physically connected to the baseband board by an USB interface and a converter, which maps the USB to the customized EPP port. Moreover, the RF performance of the front-end board can be measured individually when configured to standalone operation, which means that the board is controlled by the Spartan FPGA.

#### *3.1 Test modes and sequences*

Testing the baseband mainly consists of verifying the 802.11a signal processing and the MIMO extensions, which are executed by the baseband hardware, in comparison to their software based simulations. Because the correctness and the performance of the developed algorithms were theoretically proven and verified by simulations in [7], their correct behaviour in hardware blocks was checked at the Rx by feeding the baseband board with RF-MIMO training frames composed by several OFDM training symbols. Those OFDM symbols were initially generated in Matlab for a known MIMO channel, i.e. the solutions for the optimum vector modulator settings are known. The training frames were downloaded to an RF vector signal generator (Agilent E4438C) and used as inputs for the baseband board I- and Q-signals at the Rx. The determined vector modulator weights were successfully verified against their software based calculations. Figure 4a) shows an example of that test sequence.

Furthermore, the correct transmission and reception of 802.11a compliant frames were verified for control and data frames. For the Tx, the USB program generated beacon and data frames, which were analysed by an oscilloscope at the DACs' outputs. For the Rx direction, data frames were generated by Matlab, fed to the baseband inputs via the E4438C RF signal generator, and the frames were verified by the terminal program at MAC layer. All tests for checking the 802.11a conformance were passed successfully.

Finally, two baseband boards were directly connected at the ADCs and DACs, i.e. the RF front-end is bypassed by a "wired" link<sup>[0]</sup>. In this test scenario, different frames were successfully transmitted and received, which includes control frames, conventional 802.11a data frames, and MIMO training frames. Moreover, these tests were performed at different data rates up to 48 Mbit/s (64 QAM).

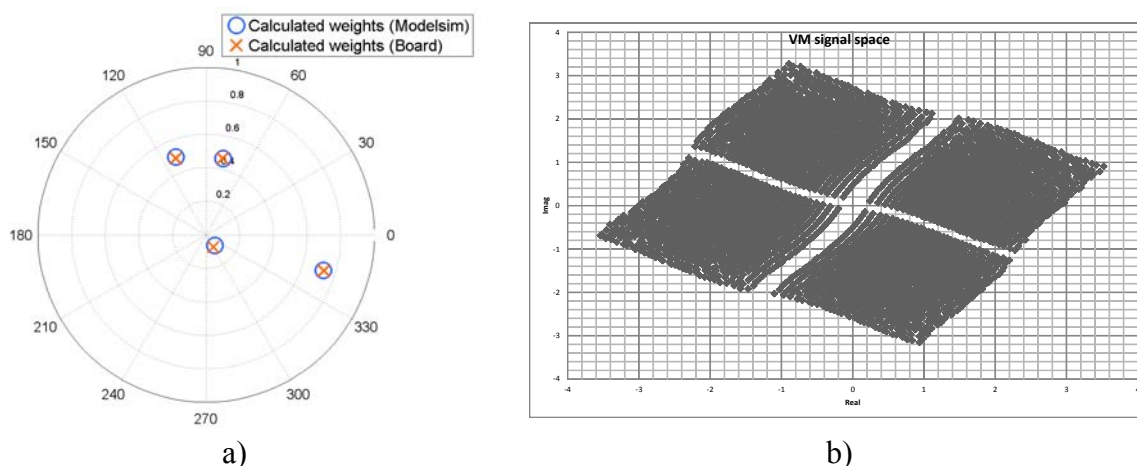


Figure 4 Verification of the physical layer for MIMO modes in 802.11a. a) Vector modulator settings from the baseband hardware for known channels. b) Vector modulator signal space.

The RF board was first tested in standalone operation, in which all components are controlled by the on-board Spartan-3 FPGA. A compliant 802.11a transmission based on the MAX2829 IC was successfully verified by test signals and data transmission, for which the MIMO modes were deactivated by selecting dedicated antennas for the Tx and the Rx. More particularly, configuring the MAXIM MAX2829 chip via the Spartan-3 or by commands from the baseband board was tested, and the RF performance was evaluated for the 802.11a mode, e.g. phase-locked loop operation, transmitted output power, etc.

The MIMO operation modes were tested at different test points, e.g. directly in the RF domain or by analysing the down-converted I- and Q-symbols at the baseband. The vector modulator settings were verified by feeding their inputs with sine waves, transferring dedicated weight settings from the FPGA to the weighting circuitry, and evaluating the outputs of those modulators. An example of the measured RF performance is shown in Figure 4b), which presents the achievable signal space of one vector modulator. The observed gaps are related to DAC mismatches in the modulators<sup>2</sup>, which are eliminated in redesigned ICs. Furthermore, the rotation of the constellation diagram does not affect the concept because this effect is related to channel responses and correctly taken into account by the baseband algorithms. Moreover, the combining of all antenna branches was verified at the Rx after the combiner by RF measurements and at the baseband outputs. In conclusion, the coexistence of 802.11a and MIMO transmission was successfully tested for the front-end board.

<sup>2</sup> Weights from the baseband are digitally stored in registers at the vector modulators and converted into analogue control voltages by means of integrated DACs.

Nevertheless, the RF MIMO concept demands for a complete system verification and performance evaluation. Figure 5 shows the prototyping setup for testing the complete physical layer with regard to its MIMO performance. The MAC protocol is emulated by a terminal program, which runs on a USB-connected PC. This terminal program allows configuring the shown system setup comprehensively, e.g. all parameter settings, sending and receiving training or normal frames, changing vector modulator settings, etc.

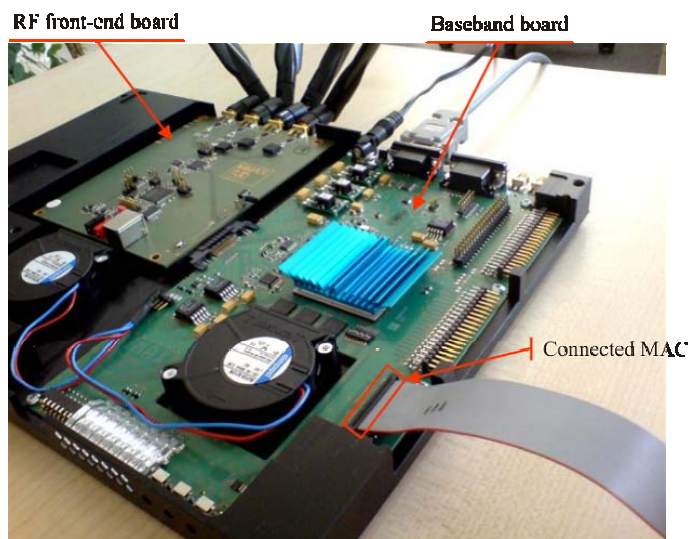


Figure 5 Baseband and front-end system assembling and test setup for rapid prototyping.

The tests for verifying the prototyping platform of the physical layer consist of verifying 802.11a legacy transmission between two stations and the MIMO operation modes, i.e. each station contains a baseband and a front-end PCB. All tests were successfully accomplished in an indoor environment. Starting with the transmission of 802.11a data frames between both stations, training frames for channel estimation were transmitted, received, and correctly decoded. Consequently, the RF-MIMO concept was verified for the complete physical layer.

### 3.2 System integration aspects

In the current system partitioning, the prototyping system is separated into three different PCBs, which allow testing and debugging each system independently from the remaining subsystems. The MAC processing hardware based on a MIPS RISC core is already designed as an application-specific integrated circuit (ASIC) in a 0.25  $\mu\text{m}$  SiGe-BiCMOS technology and assembled with an additional FPGA for hardware acceleration on a PCMCIA card. Here, the hardware accelerators can be additionally integrated into the RISC core for size and cost reduction and speed-up.

The baseband board executes its signal processing on an FPGA, but it was designed flexibly for an ASIC development. Therefore, integration with the MAC processor as a system-on-chip is feasible and reduces the overhead in interfaces between both subsystems.

In its current configuration, the RF front-end PCB contains the building blocks for RF MIMO support only at the Rx, whereas simple antenna selection is used for the Tx, i.e. only 1x4 MIMO transmission modes are supported. Redesigned Tx and Rx ICs contain all relevant circuits for enabling 4x4 MIMO operation, and they are separated into two different chips to prevent strong coupling effects between them. That front-end does not need the MAXIM chip anymore, but still uses the Spartan-3 FPGA to support standalone operation and protocol conversion of the baseband commands. Because the same interfaces and protocols are used, both board versions are exchangeable.

Finally, the highest integration is achieved by assembling the MAC processing core, the baseband processor and the RFICs on a single PCB, e.g. a PCMCIA card or similar form factor. Here, the antenna array can be connected via UFL connections and optimised for that specific geometry of the handheld device because diversity characteristics of the array, the antenna matching, and the radiator arrangement mainly depend on the available space and used materials.

#### 4. Conclusions

The architecture of a WLAN transceiver was presented, which supports additional MIMO transmission modes in coexistence with the legacy IEEE 802.11a frame format. To enable spatial diversity, RFICs were designed for weighting and combining the antenna signal already in the analogue RF domain, and algorithms for beamformer selection and channel estimation were investigated for supporting this novel front-end architecture.

The physical layer was partitioned into rapid prototyping PCBs, a baseband and a front-end PCB. At the baseband board, an FPGA was used for prototyping the developed channel estimation and beamformer algorithms. Key components of the RF front-end were designed for the Rx and assembled with an off-the-shelf WLAN IC on a front-end board, which allows 1x4 MIMO transmission modes.

After successfully verifying both subsystems independently, the complete prototyping system was validated in its functionality. Here, the coexistence of both technologies and the extension of 802.11a with MIMO modes were demonstrated, i.e. any off-the-shelf 802.11a WLAN IC can be extended for MIMO transmission. Finally, detailed performance evaluations with respect to defined performance metrics like bit error rates and its usage in mobile services like IPTV are ongoing.

#### Acknowledgement

The research leading to these results has received funding from the European Community's Seventh Framework Programme (FP7/2007-2013) under grant agreement n°213952 (MIMAX). Moreover, the authors thank IHP for manufacturing the ICs and Altium Europe for their support in PCB design.

#### References

- [1] T. K. Paul and T. Ogunfunmi, "Wireless LAN Comes of Age: Understanding the IEEE 802.11n Amendment," *IEEE Circuits and Systems Magazine*, vol. 8, pp. 28-54, 2008.
- [2] IEEE, "IEEE Std 802.11n-2009," in *IEEE Standard for Information technology - Telecommunications and information exchange between systems - Local and metropolitan area networks - Specific requirements Part 11* ed, 2009, pp. c1-502.
- [3] L. Qinghua, L. Guangjie, L. Wookbong, *et al.*, "MIMO techniques in WiMAX and LTE: a feature overview," *IEEE Communications Magazine*, vol. 48, pp. 86-92, 2010.
- [4] M. Zargari, L. Y. Nathawad, H. Samavati, *et al.*, "A Dual-Band CMOS MIMO Radio SoC for IEEE 802.11n Wireless LAN," *IEEE Journal of Solid-State Circuits*, vol. 43, pp. 2882-2895, 2008.
- [5] M. R. N. Ahmadi, L. Y. Chen, N. Fayyaz, *et al.*, "A novel CMOS integrated smart antenna transceiver," in *IEEE Radio and Wireless Symposium*, 2006, pp. 299-302.
- [6] R. Eickhoff, R. Kraemer, I. Santamaria, *et al.*, "Developing Energy-Efficient MIMO Radios," *IEEE Vehicular Technology Magazine*, vol. 4, pp. 34-41, 2009.
- [7] J. Via, I. Santamaria, V. Elvira, *et al.*, "A General Criterion for Analog Tx-Rx Beamforming Under OFDM Transmissions," *IEEE Transactions on Signal Processing*, vol. 58, pp. 2155-2167, 2010.
- [8] I. Santamaria, J. Via, A. Nazabal, *et al.*, "Capacity region of the multiantenna Gaussian broadcast channel with analog TX-RX beamforming," in *5th International ICST Conference on Communications and Networking in China (CHINACOM)*, 2010.